

DESIGN ALGORITHM FOR AUTOMATED DYNAMIC GRASPING OF LIVE BIRDS

Kok-Meng Lee, *Member, IEEE*, and Xuecheng Yin

Abstract— This paper presents a method for designing a dynamic grasper for handling natural objects (such as live birds) for subsequent processing. The dynamic grasper uses flexible fingers to accommodate a limited range of varying sizes, shapes, and some motion due to the live object's natural reaction to mechanical grasping. As compared to fingers with multiple active joints, flexible fingers have many potential advantages, because they are lightweight and they have no relative individual moving parts in each of the fingers. The advantages of flexible fingers are seldom exploited for grasping, however, because of complicated analysis involved in their design. For this reason, we present an analytical method for designing a dynamic grasper for handling natural objects on a moving conveyor.

Index terms grasping, handling, part-feeding, automation.

I. INTRODUCTION

For high-speed automated transfer of live objects from a conveyor to a moving processing line, it is often necessary to "grasp" the object in continuous motion with relatively soft fingers in order to avoid bruising the object and to minimize the object's natural response variability and struggle. For poultry processing where live birds must be transferred from conveyors to a kill-line, an additional challenge is that the grasping mechanism must be able to accommodate a limited range of varying sizes, shapes, and some motion due to the bird's natural reaction to mechanical grasping. At the same time, the grasping mechanism must be able to meet the production throughput requirement at reasonable cost.

Grasping has been addressed extensively in the literature in the past two decades. However, most robotic grasping research has assumed knowledge of object's shape, location, and orientation. Once exact object information is established, finger positions that ensure force-closure grasp are designated. Live, natural objects, however, are typically characterized by varying sizes and shapes in batch processing, and they have natural reflexes (or voluntary motion) consequently the exact position and shape are not known *a priori*. Although a number of authors (for example in Kaneko and Tanie, 1988) have directed their efforts towards grasping of an unknown object, it is assumed in many papers that the object being grasped is rigid and

stationary, and that the multi-joint fingers are typically composed of multiple links of rigid members.

Rotating rubber fingers have been used in poultry harvesters to drive broilers into cages for transportation from farms to processing plants (Kettlewell and Turner, 1985). They have recently been explored for use in singulation (Lee, 1999; Lee *et al.* 1999) and for grasping (Lee, 2000) of natural objects. As compared to fingers with multiple active joints, flexible fingers have many potential advantages because they are lightweight and they have no relative individual moving parts in each of the fingers. They can accommodate some variation in sizes/shapes and some motion due to the live object's natural reaction to mechanical grasping. The advantages of flexible fingers are seldom exploited for grasping, however, because of complicated analysis involved in their design. The contact-dependent force needed for grasping, coupled with the effect of energy storage in the flexible members and the non-linearities introduced by the large deflection, complicates the modeling and analysis. Due to these difficulties, the design of flexible fingers has been accomplished by extensive trial-and-error methods. To facilitate design of a dynamic grasper consisting of rubber fingers, a design algorithm has been developed.

The remainder of this paper is organized as follows: Section 2 gives an overview of a dynamic grasper. The geometric representation that characterized the interaction between the moving object and the rotating fingers is derived in Section 3. In Section 4, key parameters and essential equations for the design process are given. To improve readability, the development of some equations/proof is outlined in the appendix. Along with a practical design example and simulation results, Section 5 highlights the significant effects of the design parameters on the grasping. Conclusions are given in Section 6.

II. OVERVIEW OF THE DYNAMIC GRASPER

The dynamic grasper consists of a pair of rotating mechanical hands, each having n columns of evenly spaced rubber fingers. The two hands (driven by servomotors) rotate at the same speed but in opposite directions. Figure 1 shows two typical columns of a rotating hand for transferring a natural object from a moving pallet to a shackle for subsequent handling. For an appropriate choice of finger spacing, the body grasper could be designed to

The authors are with the George W. Woodruff School of Mechanical Engineering, Georgia Institute of Technology, Atlanta, GA 30332-0405. For more information, contact kokmeng.lee@me.gatech.edu

trap the bird within a matrix of twelve fingers (i.e. 2 columns of 3 rows in each of the two hands).

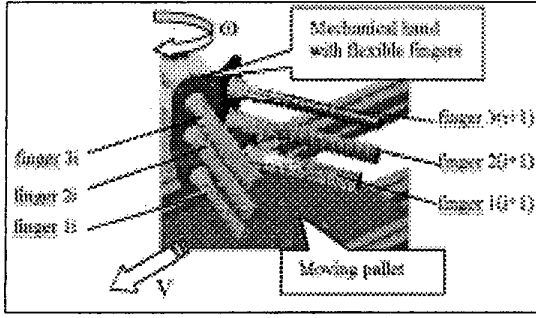


Figure 1: CAD model of a dynamic grasper

The fingers grasp the bird's body including its femur (or the thigh) while allowing the legs to freely extend downward. The first (lowest) row of fingers supports the weight of the bird; and thus these fingers are relatively harder and shorter than other rows of fingers in order to prevent them from interfering with the legs. The second row traps the body and translates the bird, and the third row prevents the bird from escaping above.

To illustrate the method of intersecting the moving object, we define the coordinate systems as shown in Figure 2. The fixed (reference) coordinate frame $C_w(XYZ)$ is assigned at the intersection between the rotating axis and the plane of the pallet, where the X- and Z-axes are in the direction of the pallet motion and along the rotating axis of the fingers respectively. The object body-coordinate frame $C_o(xyz)$ is at the geometric center of the object, where the x- and y-axes point along the length and width of the object respectively. In addition, a moving coordinate frame $C_{fi}(x_f, y_f, z_f)$ is attached at the base of the finger, where x_f and z_f are in the radial direction and parallel to Z-axis respectively.

The following assumptions are made in deriving the grasping force model:

1. The bird is modeled as an ellipsoid:

$$\frac{x^2}{\eta^2} + \frac{y^2}{\lambda^2} + \frac{z^2}{\gamma^2} = 1 \quad (1)$$

where η , λ , and γ are constants characterizing the broiler's dimensions. Equation (1) can be rewritten as

$$f(x, y, z) = P_b^T M P_b - 1 = 0 \quad (1a)$$

$$\text{where } M = \begin{bmatrix} \frac{1}{\eta^2} & 0 & 0 \\ 0 & \frac{1}{\lambda^2} & 0 \\ 0 & 0 & \frac{1}{\gamma^2} \end{bmatrix} \quad (1b)$$

and P_b is a position coordinate on the object surface

2. The bird is symmetric and constrained to move along the centerline between the two hands in the X direction. Thus, only one rotating mechanical hand (RMH) is considered. In addition, the bird's posture entering the grasper is known.

3. The hands are assumed to rotate at a constant speed ω and the bird travels at the same speed as the pallet V . Of particular interest here is to develop a method to synchronize the periodic motion of the rotating hands with respect to the bird's arrival.
4. The fingers in the lowest row are sufficiently stiff to support the weight of the bird.

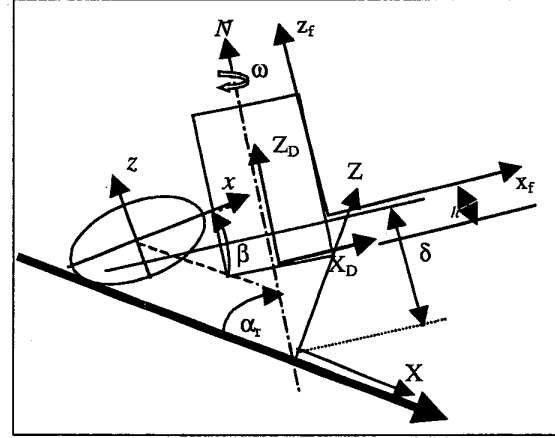


Figure 2: Coordinate frame used in derivation

III. KINEMATICS OF BIRD-FINGER INTERACTION

The equation of the ellipsoid with respect to the XYZ frame can be described by using the following transformation:

$$P_w = [R_1]P_b + P_{b0} \quad (2)$$

where $[R_1]$ and P_{b0} are the rotational matrix and the centroid of the ellipsoid with respect to C_w respectively. Similarly,

$$P_w = [R_2]P_d + P_{d0} \quad (3)$$

$$P_d = [R_3]P_{fi} + P_{fi0} \quad (4)$$

where $[R_2]$ and P_{d0} are the rotational matrix and the origin of the rotating cylinder with respect to C_w respectively; $[R_3]$ is the rotational matrix of C_{fi} with respect to C_d (a fixed coordinate frame that accounts for the inclination of the drum); and P_{fi0} is the position coordinate of the finger frame C_{fi} in C_d . Eliminating P_d and P_w from Equations (2), (3) and (4), we have

$$P_b = [R_{bfi}]P_{fi} + P_{bfi0} \quad (5)$$

$$[R_{bfi}] = [R_1][R_2][R_3] \quad (5a)$$

$$P_{bfi0} = [R_1]\{[R_2]P_{fi0} + P_{d0} - P_{b0}\} \quad (5b)$$

Substituting Equation (5) into Equation (1a), the ellipsoid can be described geometrically in the finger frame C_{fi} or

$$f_o(x_{fi}, y_{fi}, z_{fi}) = 0$$

In the rotating plane of the finger ($z_{fi}=0$), the cross-section where the ellipsoid is intercepted by the plane of rotation is essentially an ellipse in the form of Equation (6):

$$a_{11}x_{fi}^2 + 2a_{12}x_{fi}y_{fi} + a_{22}y_{fi}^2 + 2a_1x_{fi} + 2a_2y_{fi} + a_3 = 0 \quad (6)$$

Equation (6) can be written in a standard form using the derivation outlined in the appendix:

$$\frac{(x_{fi} - x_{co})^2}{\eta_e^2} + \frac{(x_{fi} - y_{co})^2}{\lambda_e^2} = 1 \quad (7)$$

where η_e and λ_e the equivalent major and minor radii of the ellipse respectively; and (x_{co}, y_{co}) define the center of the ellipse in the finger frame C_{η} .

IV. DESIGN EQUATIONS OF THE GRASPING

Figure 3 shows the relationship between the fingers with respect to the ellipse as viewed in the normal to the plane of finger rotation. Any point on the i^{th} finger can be described in the object coordinate frame by Equation (8):

$$\begin{bmatrix} x_{ci} \\ y_{ci} \end{bmatrix} = r \begin{bmatrix} \cos(\omega t + \phi_i) \\ \sin(\omega t + \phi_i) \end{bmatrix} - \begin{bmatrix} X_{co} + Vt \\ Y_{co} \end{bmatrix} \quad (8)$$

where $r_o \leq r \leq r_o + \ell$; $\phi_i = (i-1)\phi_a$ denotes the initial angular position of i^{th} finger; (X_{co}, Y_{co}) define the initial position of the ellipse in XYZ frame at $t=0$; ϕ_a is the included angle between two adjacent columns; r_o is the radius of the drum; and ℓ is the length of the finger.

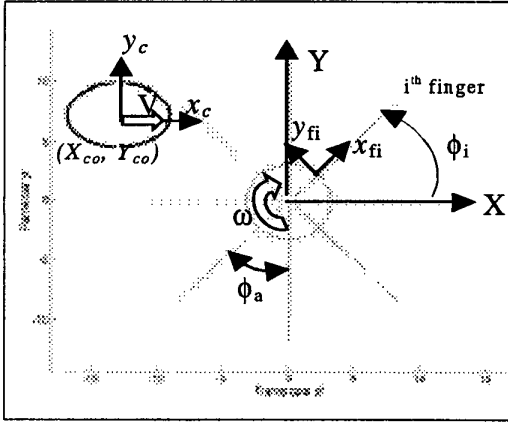


Figure 3: Bird-finger relationship

A. Grasping configuration

Equation (8) shows that the i^{th} finger repeats every $2\pi \frac{V}{\omega}$ along the x -axis, as viewed in the bird's coordinate frame. In addition, when $\phi_i + \omega t = \frac{\pi}{2}$, the x_f axis of the finger is parallel to the y -axis; and the corresponding distance between the x_f axis of the i^{th} finger and the y -axis is given by

$$x_{iy} = -[X_{co} + \frac{V}{\omega}(\phi_i - \frac{\pi}{2})]; \quad (9)$$

and the motion of the fingers can be treated as a periodic signal in x with a period equal to

$$x_p = \frac{V}{\omega} \phi_a. \quad (10)$$

The specific grasping configuration (or the number of fingers simultaneously in contact with the object) depends

on the parameters x_{iy} and x_p , where for a specified linear-angular speed ratio $\frac{V}{\omega}$, the former is a function of the bird's arrival X_{co} , and the latter depends on the design parameter ϕ_a .

B. Intercepting the moving object

In order to trap the moving object between a pair of fingers as the hand rotates relative to the object, we design the i^{th} finger to intercept the object at $x_{ci} = \eta_e$ and $y_{ci} = 0$ at $t = t_i$, and the $(i+1)^{\text{st}}$ finger to grasp the object at $x_{c(i+1)} = x_d$ and $y_{c(i+1)} = y_d$ at $t_{i+1} = t_i + \Delta t$. Note that (x_d, y_d) must be in the third quadrant of the ellipse's perimeter, otherwise the $(i+1)^{\text{st}}$ finger may slip past the bird.

To solve for the time t_i needed for the i^{th} finger to touch the moving object at the initial location X_{co} , we substitute $y_{ci} = 0$ and $x_{ci} = \eta_e$ into the y - and x -components of Equation (8), which leads to

$$t_i = \frac{1}{\omega} \sin^{-1} \left(\frac{Y_{co}}{r_o + \ell} \right) - \phi_i \quad (11a)$$

$$X_{co,i} = -\sqrt{(r_o + \ell)^2 - Y_{co}^2} - (\eta_e + Vt_i) \quad (11b)$$

Similarly, to solve for the time t_{i+1} needed for the $(i+1)^{\text{st}}$ finger to contact the object at the desired location $x_{c(i+1)} = x_d$ and $y_{c(i+1)} = y_d$, we have from Equation (8):

$$\begin{bmatrix} x_d \\ y_d \end{bmatrix} = r_{i+1} \begin{bmatrix} \cos(\omega t_{i+1} + \phi_{i+1}) \\ \sin(\omega t_{i+1} + \phi_{i+1}) \end{bmatrix} - \begin{bmatrix} X_{co,i+1} + Vt_{i+1} \\ Y_{co} \end{bmatrix} \quad (12)$$

where $t_{i+1} = t_i + \Delta t$; Δt is the additional time required by the $(i+1)^{\text{th}}$ finger to intercept the object. Since $X_{co,i+1} - X_{co,i} = V\Delta t$ and $\phi_{i+1} = \phi_i + \phi_a$, the design parameters $(\phi_a, \Delta t)$ can again be found from Equation (8):

$$\phi_a = \sin^{-1} \left(\frac{Y_{co} + y_d}{r_{i+1}} \right) - \sin^{-1} \left(\frac{Y_{co}}{r_o + \ell} \right) - \omega \Delta t \quad (12a)$$

where

$$\Delta t = \frac{1}{2V} \left[\sqrt{(r_o + \ell)^2 - Y_{co}^2} + \eta_e - \sqrt{r_{i+1}^2 - (y_d + Y_{co})^2} - x_d \right] \quad (12b)$$

C. Grasping force prediction

When the rotating finger is in contact with an object, the reaction force f causes the finger to deflect. The deflection of the finger depends on the coefficient of friction at the contact interface, the object geometry, the shape of the deflected finger, and the location at which the force is applied. The rotating finger is treated as "quasi-static" and solved approximately using static mechanics. In the case, the equations of static mechanics can be applied at each instant in time as though the deflected finger were in static equilibrium:

$$\mu = \frac{f_t}{f_n} = \tan(\alpha + \psi_o - \frac{\pi}{2}); \quad (13)$$

where μ is the coefficient of friction between the finger and the object; f_t and f_n are the tangential and normal components of the contact force perpendicular to and along the finger at the contact point respectively; α defines the direction of the contact force acting on the finger; and ψ_o is the slope of finger at the contact point.

The location and the slope of the object at the contact point must satisfy the following equations:

$$f_o(x = x_i, y = y_i) = 0 \quad (14a)$$

$$\left. \frac{\frac{\partial f_o(x,y)}{\partial y}}{\frac{\partial f_o(x,y)}{\partial x}} \right|_{(x=x_i, y=y_i)} = \tan \psi_o \quad (14b)$$

where $f_o(x, y) = 0$ describes the geometry of the object.

For a given force f exerted at a known location L and direction α , the deflected shape of the finger can be modeled as a bent elastic rod as given in the form (Frisch and Fay, 1962; Lee *et al.*, 2001):

$$kx = f_1(\alpha, \psi_o) \quad (15a)$$

$$ky = f_2(\alpha, \psi_o) \quad (15b)$$

where $k = \sqrt{\frac{EI}{L^3}}$; E is the Young's modulus; I is the moment of inertia of the finger;

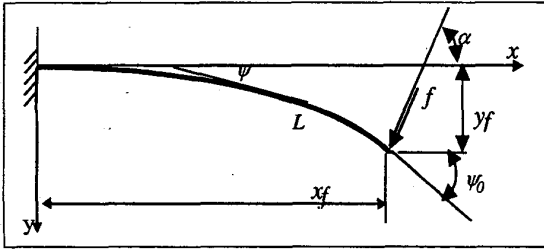


Figure 3 Model of a bent flexible finger

As the contact point and the reaction from the object are not known *a priori* in grasping, five unknowns, x_i , y_i , ψ_o , f , and α , must be solved simultaneously from Equations (13), (14a), (14b), (15a) and (15b). The procedure for computing the contact point and forces is illustrated by the flowchart given in Figure 4.

V. SIMULATION RESULTS

An algorithm has been written using MATLAB to serve the following functions: (1) Help visualize the effect of design changes. (2) Provide a means to examine the sensitivities of the design parameters. (3) Facilitate the decision-making in the design process.

Figure 5 shows a snap shot of the rotating fingers, where 2 and 3 denotes the planes of finger's rotation and deflection respectively. To provide clarity, only the deflection of one finger (marked as 1) is shown.

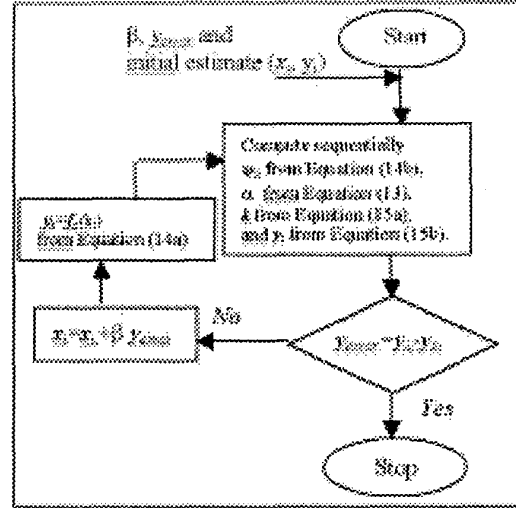


Figure 4: Flowchart illustrating the computational procedure

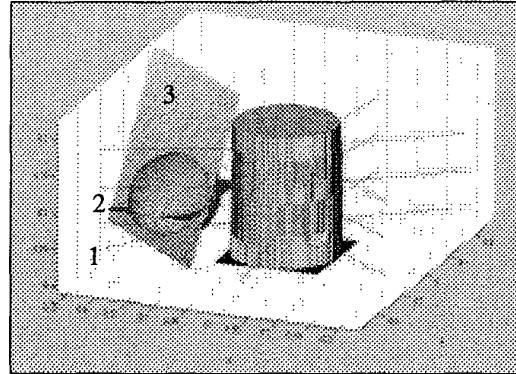


Figure 5 Bird-finger interaction in 3-D. (1: deflected finger; 2: plane of finger rotation; 3: plane of the finger deflection)

A. Effects of the design parameters on initial interception

Table 1 lists a set of typical values used in the following illustration. Figure 6 shows the typical loci of the three consecutive un-deflected fingers (or the x_f axis) as viewed in the object coordinate frame.

Table 1: Illustrative parameters

V = 0.508 m/s (20 in.); $\omega = 20$ rpm (2.09rad./s); $30^\circ < \phi_a \leq 45^\circ$			
Bird size	Minimum	Mean	Maximum
η_e , m (in.)	0.075 (2.94)	0.099 (3.9)	0.116 (4.56)
λ_e , m (in.)	0.049 (1.93)	0.067 (2.65)	0.077 (3.02)
X_o , m (in.)	-0.463 (-18.22)	-0.487 (-19.19)	-0.504 (-19.85)

The significances of the two design parameters (x_{iy} and x_p) can be summarized as follows:

- Figure 6 shows that the object moves between two columns of fingers for a specified x_{iy} and x_p . Note that if x_{iy} is too small (see, for example, the 5th column

with $x_{iy} = 0$), the object may be in contact with only one column of fingers as it moves with respect to the rotating hand.

- Recall that the motion of the fingers is periodic in x . Thus, the four unknowns (x_d , y_d , Δt , and ϕ_a) can be estimated by solving simultaneously Equations (12), (14a) and (14b) in the range $[x_{iy} - x_p, x_{iy} + x_p]$.
- From Equations (9) and (10) along with the aid of Figure 6, the appropriate range of ϕ_a can be estimated to be $30^\circ \leq \phi_a \leq 45^\circ$ for the given range of bird sizes.

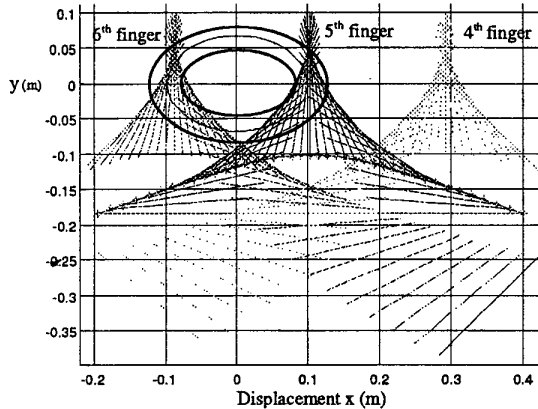


Figure 6: Illustration of grasping configuration

B. Effects of the design parameters on grasping force

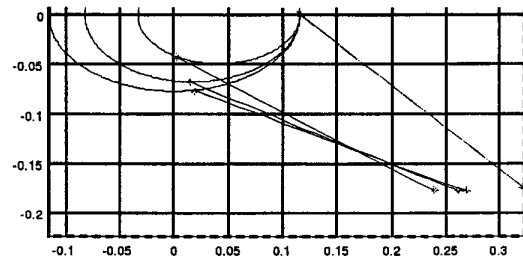
The two design configurations, $\phi_a = 30^\circ$ and $\phi_a = 45^\circ$, are compared in Table 2 where the maximum grasping forces are summarized. As compared in Table 2, the contact force increases as ϕ_a decreases. In other words, reducing x_p has the effect of increasing the grasping force for a fixed speed ratio $\frac{V}{\omega}$.

Table 2: Maximum contact force (N)

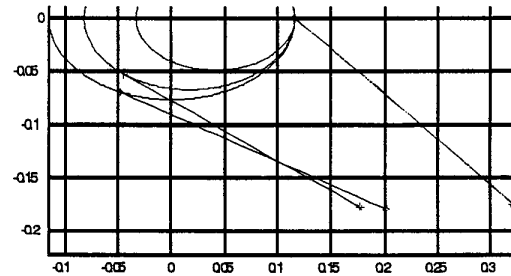
Bird Size	5 th finger	6 th finger	
		$\phi_a = 45^\circ$	$\phi_a = 30^\circ$
Minimum	3.518	0	11.8
Mean	4.913	11.23	37.21
Maximum	5.688	33.293	85.1

Figure 7 illustrates the initial interceptions at the instants t_i and t_{i+1} . If x_p (or ϕ_a for a constant speed ratio) is too small, the $(i+1)^{\text{st}}$ finger intercepts the ellipse in its fourth quadrant, and it could slip pass the bird as shown in Figure 7(a) where $\phi_a = 30^\circ$. On the other hand, the $(i+1)^{\text{st}}$ finger may miss some of the smaller birds if x_p is too large as illustrated in Figure 7(b) where $\phi_a = 45^\circ$. Using the design algorithm, an acceptable x_p has been determined, which led to $\phi_a = 43.3^\circ$ for the given speed ratio and the range of bird sizes as shown in Figure 7(c). The corresponding

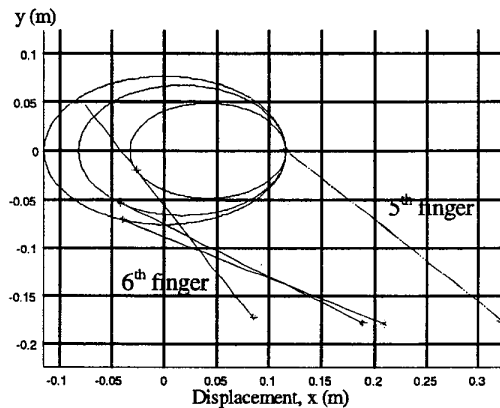
trajectories of deflected fingers and contact forces on the bird are displayed in Figure 8. Figure 8(a) shows the force vectors and the contact points on the deflected fingers as the bird is transported. The corresponding force vectors and contact points on the bird are given in Figure 8(b). As shown in Figure 8(c), where the resultant forces of both fingers #5 and #6 are plotted as a function of time, the process can be broadly divided into three regions; namely engaging, trapping and discharging. To allow time to manipulate both legs of the bird, it is desired to maximize the trapping time while minimizing the forces on the bird.



7(a) $\phi_a = 30^\circ$



7(b) $\phi_a = 45^\circ$



7(c) $\phi_a = 43.3^\circ$

Figure 7: Configuration at initial interception

ACKNOWLEDGEMENT

The Agriculture Technology Research Program (ATRP) and the U.S. Poultry and Egg Association have supported this project.

REFERENCES

Kaneko M. and K. Tanie, (1988) Basic considerations on the development of a multi-fingered robot hand with the capability of compliance control, in Proc. Advances in Robot Kinematics, Ljubljana, , pp. 46-52.

Kettlewell, P. J. and M. J. Turner, 1985, A Review of Broiler Chicken Catching and Transport Systems, Journal of Agricultural Engineering Research, (1985)31, pp. 93-114.

Korn, G. and T. Korn, (1968) Mathematical Handbook for Scientist and Engineers, McGraw-Hill (2nd Edition) pp 76.

Lee, K.-M., 1999, "On The Development of a Compliant Grasping Mechanism for on-Line Handling of Live Objects, Part I: Analytical Model," IEEE/ASME Int. Conf. on Advanced Intelligent Mechatronics (AIM'99), Atlanta, GA, Sept. 19-23.

Lee, K.-M., A. B. Webster, J. Joni, X. Yin, R. Carey, M. Lacy, R. Gogate, 1999, "On The Development of a Compliant Grasping Mechanism for On-Line Handling of Live Objects, Part II: Design and Experimental Investigation," AIM'99, Atlanta, GA, September 19-23.

Lee, K.-M., 2000, Design Criteria for Developing an Automated Live-bird Transfer System, IEEE ICRA 00, San Francisco, April 22-28.

Lee, K.-M., J. Joni, and X. Yin 2001, Compliant Grasping Force Modeling for Handling of Live Objects, IEEE/ICRA 01, Seoul, Korea, May 21-26.

Appendix: Ellipse in Standard form

To transform Equation (6) into a standard equation of ellipse, we introduce the following transformation:

$$\mathbf{x} = [\bar{v}_1 \quad \bar{v}_2] \mathbf{x}_c \quad (\text{A.1})$$

where $[\bar{v}_1 \quad \bar{v}_2]$ are the eigenvectors of $\rho_2 = \begin{bmatrix} a_{11} & a_{12} \\ a_{12} & a_{22} \end{bmatrix}$.

The eigenvalues are

$$\lambda_{1,2} = \frac{(a_{11} + a_{22}) \pm \sqrt{(a_{11} - a_{22})^2 + 4a_{12}^2}}{2} \quad (\text{A.2})$$

If $(a_{11} - a_{22})^2 + 4a_{12}^2 > 0$, then the eigenvalues are real and the corresponding eigenvectors can be shown to be

$$\bar{v}_1 = \frac{1}{D} \begin{bmatrix} -a_{12} \\ \lambda_1 \end{bmatrix} \quad (\text{A.3a})$$

and

$$\bar{v}_2 = \frac{1}{D} \begin{bmatrix} -2a_{12} \\ \lambda_2 \end{bmatrix} \quad (\text{A.3b})$$

where

$$D = \frac{1}{2} \sqrt{4a_{12}^2 + 2(a_{11} - a_{22})^2 + 2(a_{11} - a_{22})\sqrt{(a_{11} - a_{22})^2 + 4a_{12}^2}}$$

Substituting Equation (A.1) into Equation (6) leads to

$$\lambda_1 x_c^2 + \lambda_2 y_c^2 + b_1 x_c + b_2 y_c + a_3 = 0 \quad (\text{A.4})$$

where $b_1 = a_1 v_{11} + a_2 v_{12}$, and $b_2 = a_1 v_{21} + a_2 v_{22}$.

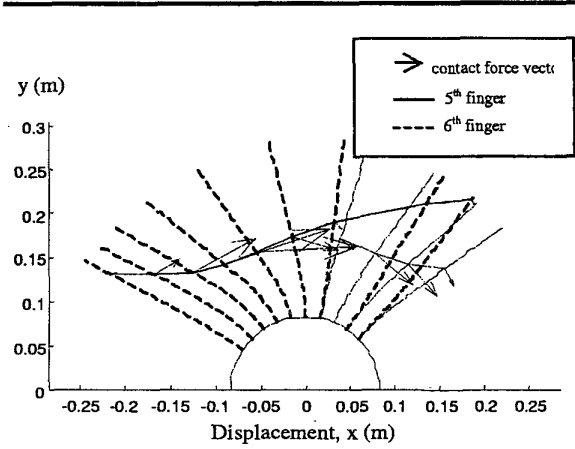
Equation (A.4) can be written as

$$\frac{(x_c - x_{co})^2}{a_c^2} + \frac{(y_c - y_{co})^2}{b_c^2} = 1 \quad (\text{A.5})$$

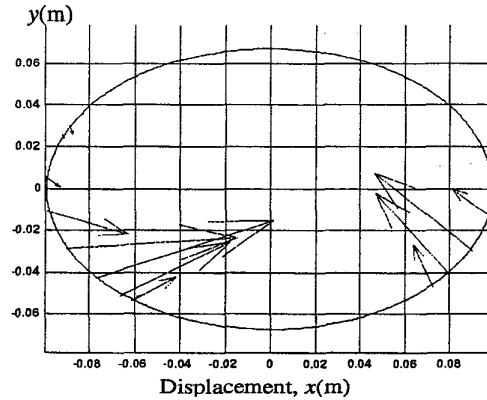
$$\text{where } a_c^2 = \frac{1}{\lambda_1} [x_{eo}^2 + y_{eo}^2 - a_3]; \quad (\text{A.6a})$$

$$b_c^2 = \frac{1}{\lambda_2} [x_{eo}^2 + y_{eo}^2 - a_3]; \quad (\text{A.6b})$$

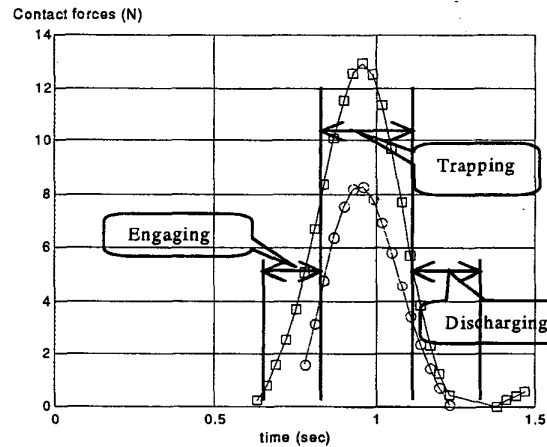
$$x_{eo} = \frac{b_1}{2\lambda_1}; \text{ and } y_{eo} = \frac{b_2}{2\lambda_2} \quad (\text{A.6c})$$



8(a) Trajectory of the deflected finger



8(b) Contact force on the bird



8(c) Contact force trajectory

Figure 8: Grasping force